Research Article – Vol. 01, Issue 03, No. 02

Advanced in Engineering and Intelligence Systems

Journal Web Page: https://aeis.bilijipub.com

Estimation of fresh and hardened properties of self-compacting concrete by optimized radial basis function methods

David Cadasse[1,*] , Antonio Fontana[2]

[1] *The King's School, BP1560, Bujumbura, Burundi*
[2] *Univ Modena & Reggio Emilia, Dept Engn Enzo Ferrari, Modena, Italy*

Highlights

- The RBFNN approach was used to predict the mechanical characteristics of SCC
- The AOA and GOA are used to optimize determinative variables in the RBFNN model
- Results of AOA-RBFNN are superior to those of GOA-RBFNN and the literature
- Regarding V-funnel outcomes, literature and GOA-RBFNN show relatively better performance

Article Info

Received: 14 July 2022
Received in revised: 18 September 2022
Accepted: 18 September 2022
Available online: 01 October 2022

Keywords

SCC;
Fly ash;
Rheological properties;
Compressive strength;
Radial basis function neural network;
Optimization algorithms

Abstract

Most of the published literature on concrete containing fly ash was limited to predicting the hardened concrete properties. It is understood that exist so restricted studies focusing on forecasting both fresh and hardened properties of self-compacting concrete (SCC). Hence, it is attempted to develop some models to predict the fresh and hardened properties of SCC by the optimized radial basis function neural network (RBFNN) method. This study aims to specify RBFNN method key parameters using arithmetic optimization algorithm (AOA) and grasshopper optimization algorithm (GOA). The considered properties of SCC in the fresh phase are the L-box test, V-funnel test, slump flow, and in the hardened phase compressive strength. The results present powerful workability during the prediction process. It is observed that the developed models have performance evaluation indices in reasonable value in the learning and testing section. All in all, the RBFNN model developed by AOA outperforms others, with R^2 values at 0.9607 (slump flow), 0.9651 (L-box), 0.9905 (V-funnel test), and 0.9934 (compressive strength), which depicts the capability of this algorithm for determining the optimal parameters of the RBFNN, While, it is worth mentioning than the model developed with GOA algorithm is also powerful.

Nomenclature

AOA	*Arithmetic optimization algorithm*	*GOA*	*Grasshopper optimization algorithm*
B	*Dosage of binder content*	*LB*	*L-box*
CAG	*Coarse aggregate*	*RBFNN*	*Radial basis function neural network*
CS	*Compressive strength*	*SP*	*Superplasticizer*
DF	*D flow*	*SCC*	*Self-compacting concrete*
FA	*Fly ash*	*VF*	*V-funnel*
FAG	*Fine aggregate*	*W/B*	*Water to binder ratio*

1. Introduction

Self-compacting concrete (SCC) was first extended in Japan, in 1988, where this concrete is an effective type of concrete blend all over the world [1]. SCC is a type of concrete which could flow the formatting and load without any exterior power. As well, it has the capability to strengthen by weight of its own [2]. The two original criteria were originally focused by the design mix, to wit the need of the big value of better particle and urgency of high-performing water decreasing mixture. Compared to

* Corresponding Author: David Cadasse
Email: davidcadasse@ksu.edu.bi

different common concrete, it needs comparatively minor human attempts that are an added benefit. As well, it increments output level and decreases noise disorders. Many explore articles are being performed in the SCC technology zone; several of these explores suggest finer increment and continuity. Alongside of all these benefits, SCC has several minus parts. The expense of output of SCC is able to be 2-3 chances bigger than normal concrete. Hence, to lower the expense, several various mixtures like metakaolin, fly ash (FA), limestone filler, ground-granulated blast-furnace slag, and ground clay bricks are able to be used [3]. These components that are utilized actions as a suitable replacement for Portland cement [4]–[9]. To extend SCC, three various criteria are required to be carried out, like filling capability, passing capability, separation resistance. Then, to meet out these needs, some test experiments are required to be carried out. Many questions occur that SCC is affordable and expense-effective.

Nowadays, the successful applications of the artificial neural network in different filed of civil engineering have been reported adapted from experimental results [10]–[13]. This usage is widely-expanded in the concrete industry to predict different properties of concrete. Oxcan et al. [14] carried out comparative research considering two methods, with ANN and fuzzy logic, to predict the CS of concrete with silica fume. For analogous usages, several of the different scholars as well as suggested appropriate samples inspired by Fuzzy and adaptive neuro-fuzzy inference system (ANFIS) to compute the CS [15]–[18]. Newly, Sonebi et al. [19] studied the new attributes of SCC utilizing SVR proceed. The outcome was affirmative and incentive that presents finer filling and passing capability. Analogous study work was as well as performed by various scholars to forecast compressive strength of concrete utilizing SVR [20]–[22]. Liu [23] considered the possibility of utilizing an SVM sample to specify autogenous shrinkage of concrete admixtures. Reciprocally, Yang [24] carried out empirical research on corroded reinforced concrete. Other papers are also developed different models to predict the properties of SCC, such as the ANN technique [15], M5' and MARS based prediction models [25], and support vector regression approach [26] for predicting the slump flow, the L-box ratio, the V-funnel time and the compressive strength. Recently, new articles have been developed with the similar aim this article using SVR and RBF networks optimized with ant-lion optimizer (ALO) and biogeography-based optimizer (BBO) with great accuracy and reliable performance [27] _ [28].

According to the aim of this study about using radial basis function neural network (RBFNN) as well as newly developed optimization algorithms, it is worth discussing this object [29]–[33]. The CS of SCC containing FA was predicted using hybrid biogeography-based optimization (BBO) with fuzzy RBFNN. The results strongly presented that the developed hybrid model has the acceptable performance to predict the CS of SCC with FA [34]. Another study concentrated on predicting the CS of SCC containing Class F FA using a hybrid model of the RBFNN and firefly optimization algorithm (FOA). The results depict that the CS predicted by the proposed models have appropriate performance in comparison with the experimental results [35].

However, most of the published articles on concrete is limited just for forecasting the hardened characteristics of concrete. It is obtained from the articles that there were so restricted researches concentrating on predicting of both fresh or hardened properties of SCC by the hybrid RBFNN method. Hence, it is tried to develop models for predicting the fresh and hardened properties of SCC by the RBFNN method. The aim of selecting AOA and GOA algorithms for optimization goals was because they developed newly and its capability and disadvantages have not been found out exactly. Also, developed RBFNN structures optimized with AOA and GOA have not been proposed so far for predicting the properties of the SCC. The RBFNN method has key parameters that can be optimized with optimization algorithms, where this study aimed to determine them using arithmetic optimization algorithm (AOA), and grasshopper optimization algorithm (GOA). To this main, experimental data observations were collected from literature for developing the GOA-RBFNN and AOA-RBFNN models. The considered properties of SCC in the fresh phase are the L-box test, V-funnel test, slump flow, and in the hardened phase in CS.

2. Materials and Methods

2.1.Data Description

The present study goaled to explore different models for predicting the output variables related to fresh and hardened properties of SCC. Many numbers of the literature have been worked with a limitation of assessing a single output property of concrete using a large number of datasets. Hence, in this study, four properties of SCC such as slump flow, L-box, V-funnel, and compressive strength are considered as output. To this aim, a dataset has been made by collecting 114 SCC samples [36]–[48]. The input variables include components of concrete: (a) binder content (B), (b) fly ash percentage (FA), (c) water to binder ratio (W/B), (d) fine aggregate (FAG), (e) coarse aggregate (CAG) and (f) super plasticizer dosage (SP). The dataset was divided at 70% for training data and the rest (30%) for testing phase [49]. Statistical parameters of the dataset as well as their histogram plots, are presented in Table1 and Fig. 1.

Table 1. Statistical parameters of variables

Category	Parameter	Input variable						Output variable			
		B	FA	W/B	FAG	CAG	SP	DF	LB	VF	CS
Train	Min.	370	0.0	0.26	656	590	0.74	510	0.6	2	23
	Max.	733	60	0.45	1010	935	21.84	810	1.0	19.2	86.8
	St. D.	73.4506	15.74	0.061	92.54	120.486	4.703	53.321	0.084	4.047	17.408
	Var.	5394.99	247.67	0.004	8563.65	14517.02	22.12	2843.14	0.007	16.378	303.07
	Range	363	60	0.19	354	345	21.1	300	0.4	17.2	63.8
	Skew.	0.0869	-0.288	-0.406	-0.272	-0.0644	0.677	-0.0457	-0.52	0.493	0.4955
	Kurt.	0.4472	-0.575	-1.059	-1.1257	-1.5461	0.494	0.3045	0.1314	-0.289	-0.908
Test	Min.	400	0.0	0.27	686	590	0.86	480	0.6	2.5	17
	Max.	628	60	0.45	1038	926	19.53	770	1	14.5	82.9
	St. D.	64.463	17.941	0.057	77.842	121.657	4.518	60.735	0.109	3.243	17.251
	Var.	4155.556	321.89	0.0033	6059.42	14800.36	20.411	3688.79	0.0120	10.5166	297.59
	Range	228	60	0.18	352	336	18.67	290	0.4	12	65.9
	Skew.	-0.5276	0.3895	-0.626	-0.219	0.2066	0.496	-0.1246	-0.799	0.1133	0.454
	Kurt.	-0.5108	-0.555	-1.055	-0.0220	-1.5411	0.2141	0.8255	0.1453	-1.1721	-0.526

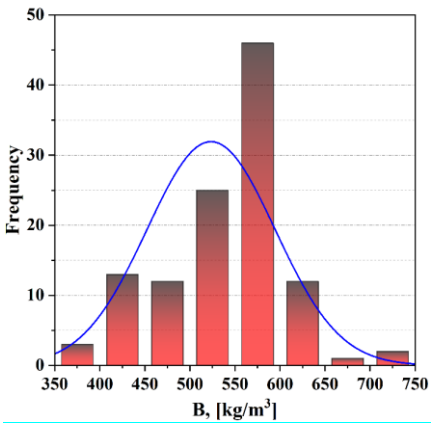

(A-1)

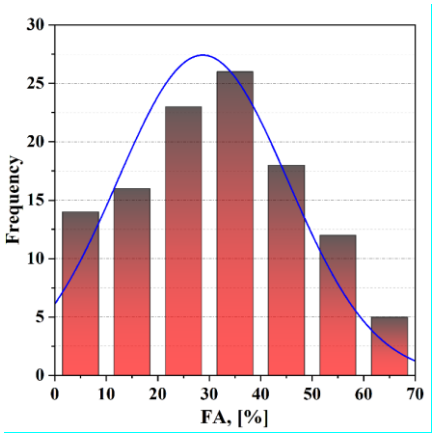

(A-2)

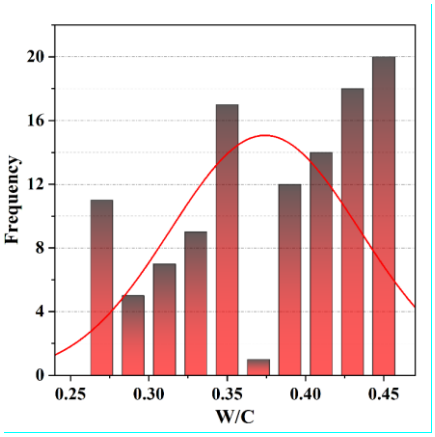

(A-3)

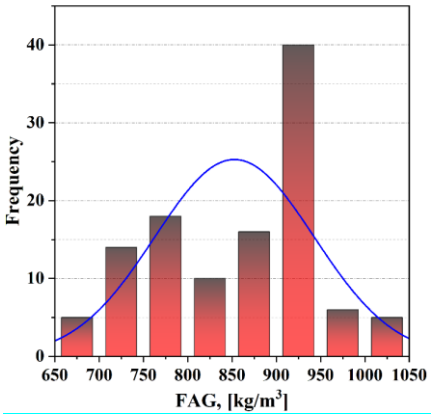

(A-4)

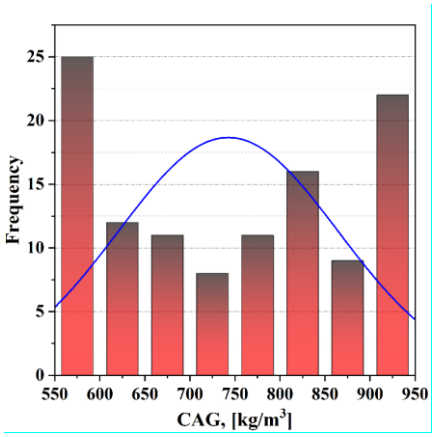

(A-5)

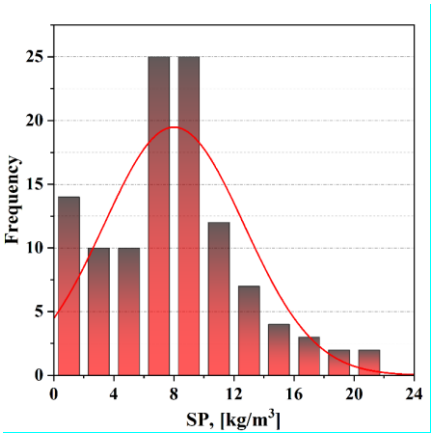

(A-6)

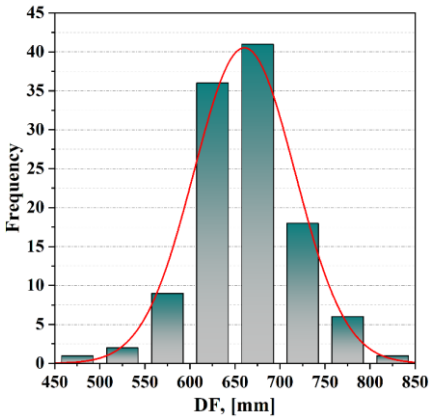

(B-1)

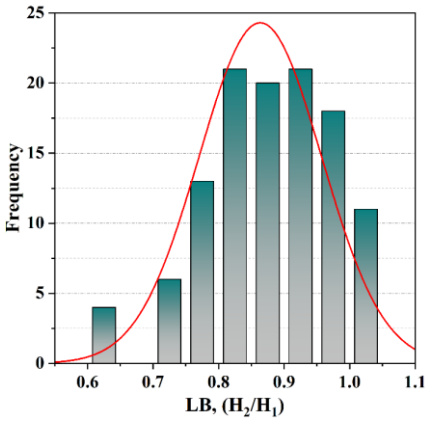

(B-2)

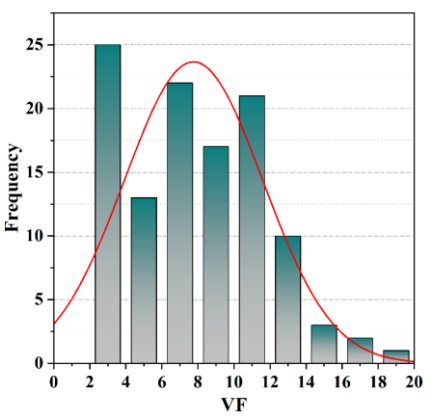

(B-3)

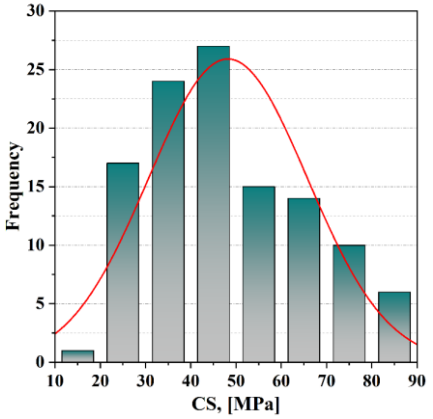

(B-4)

Fig. 1. The histogram plots of the input and output variables

2.2. Equality constraints

Arithmetic optimization algorithm (AOA) is a novel method that utilized with the conception of algebra and analysis [50]. This optimization algorithm is a metaheuristic method contains two main steps, including exploitation and exploration explaining as below. This process (shown in Eq (1)) starts by an assemblage of candidate answers (i.e., X), were produced randomly and, in every iteration, the finest candidate result is accepted as the best-gained answer or roughly the optimum since.

$$X = \begin{bmatrix} x_{1,1} & \cdots & x_{1,j} & x_{1,n-1} & x_{1,n} \\ x_{2,1} & \cdots & x_{2,j} & \cdots & x_{2,n} \\ \vdots & \ddots & \vdots & \ddots & \vdots \\ x_{N-1,1} & \cdots & x_{N-1,j} & \vdots & x_{N-1,n} \\ x_{N,1} & \cdots & x_{N,j} & x_{N,n-1} & x_{N,n} \end{bmatrix} \quad (1)$$

The math optimizer accelerated (MOA) term, is computed by Eq (2) is utilized in the search phrases.

$$MOA(C_{Iter}) = Min + C_{Itr} \times \left(\frac{Max - Min}{M_{Iter}}\right) \quad (2)$$

where $MOA(C_{Iter})$ depict a function value in the t^{th} iteration. M_{Iter} is the maximum iteration numbers, and C_{Iter} is between $[1\ to\ M_{Iter}]$ the current iteration. Min and Max point out the minimum and maximum values of the accelerated function, respectively.

The simplest rule that can create the behavior of Arithmetic operators is applied. The following location updating calculations for the searching segments.

$$x_{i,j}(C_{Iter}+1) = \begin{cases} best(x_j) \div (MOP + \varepsilon) \times \left((UB_j - LB_j) \times \mu + LB_j\right) & r_2 < 0.5 \\ best(x_j) \times MOP \times \left((UB_j - LB_j) \times \mu + LB_j\right) & Otherwise \end{cases} \quad (3)$$

In this equation, $x_i(C_{Iter}+1)$ is the i^{th} answer in the next step, $x_{i,j}(C_{Iter})$ express the j^{th} location of the i^{th} answer, and $best(x_j)$ depict the j^{th} position in the best answer. Also, ε express a tiny number, UB_j and LB_j the upper and lower bound of the j^{th} position, respectively. Here, μ is control parameter to adjust the looking procedure, can be obtainable by 0.5 according to the issue evaluated.

$$MOP(C_{Iter}) = 1 - \frac{C_{Itr}^{1/a}}{M_{Itr}^{1/a}} \quad (4)$$

where Math Optimizer Probability (MOP) is a coefficient, $MOP(C_{Iter})$ defines the value of the function at the t^{th} step, and C_{Iter} is the present step and M_{Iter} the maximum iteration. α clarifies an insightful parameter and characterizes the exploitation precise over the steps, is set to 5. The searching step is conditioned via the MOA for the condition of r_1 is not larger than the present $MOA(C_{Iter})$ value (Eq 5). In this algorithm, the exploitation operators of AOA express the search regions in depth on large dense fields and utilize two pivotal search methods to cooperate a most suitable answer that is modelled. Fig. 2 present the flowchart of AOA algorithm.

$$x_{i,j}(C_{Iter}+1) = \begin{cases} best(x_j) - MOP \times \left((UB_j - LB_j) \times \mu + LB_j\right) & r_3 < 0.5 \\ best(x_j) + MOP \times \left((UB_j - LB_j) \times \mu + LB_j\right) & Otherwise \end{cases} \quad (5)$$

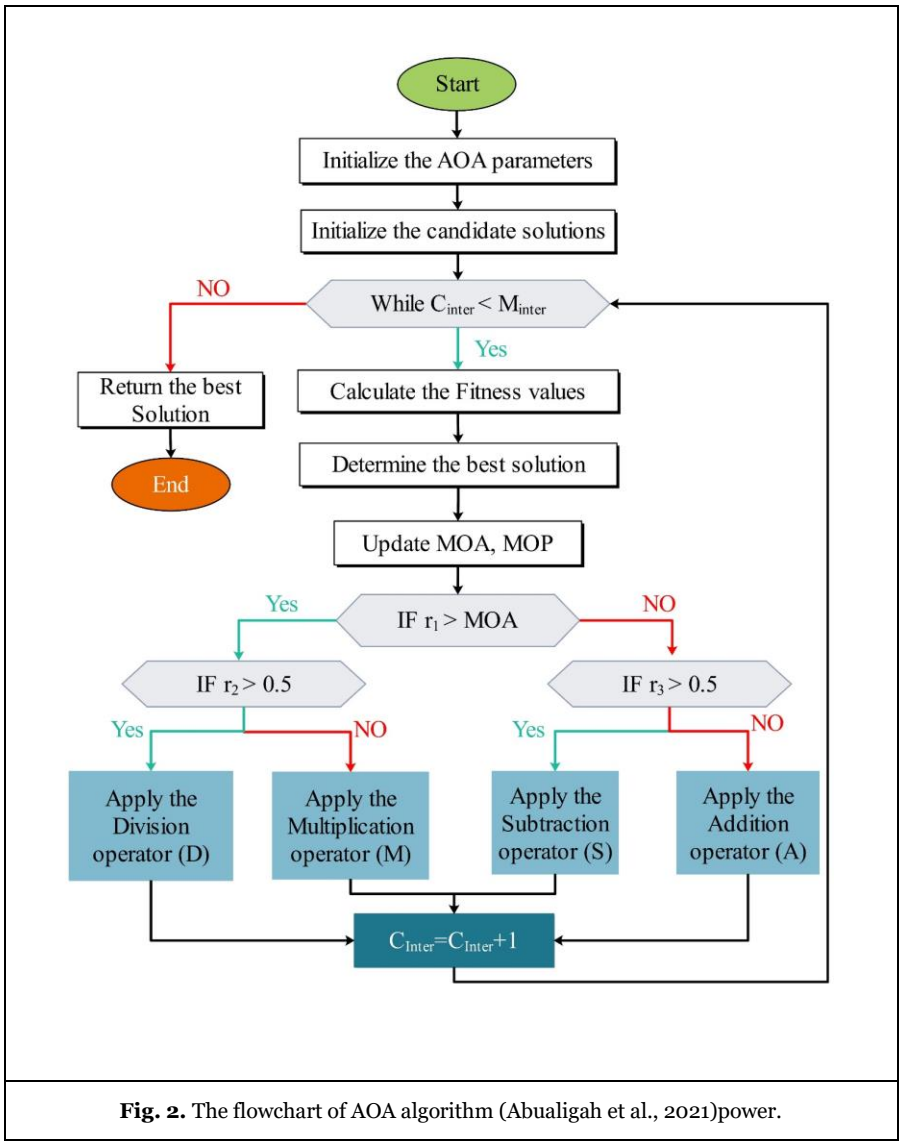

Fig. 2. The flowchart of AOA algorithm (Abualigah et al., 2021)power.

2.3. Grass hopper optimization algorithm

Grasshoppers may be found freely or in a swarm in the nature. These insects are known as feeding ones. It is worth noting that locusts are considered as a pet in which it seriously damages pastures and crops [51]. The idea of GOA is derived from the natural behavior of locust pests, which was created to find a solution to the search for optimization problems [52]. Like the previously proposed algorithms such as the whale optimization algorithm, ant lion optimizer, Salp swarm algorithm etc. this optimization is performed according to two main steps.

The initial stage is exploration step and the second one is exploitation. GOA is derived from the grasshoppers' treatment, mentioned steps are carried out to search for food source. In the exploitation phase, flying locally over the search space is responsible of the agents [52]. The treatment of the relations for various levels of some method parameters was explored for the distance between two insects, the excretion happens in this interval [53]. As a result, if the grasshoppers' distance is outside this distance, it indicates that the intended insect is going to a calming area. In conclusion, the grasshoppers are far outside this distance, indicating that the insect is going to a calm area. The movement of grasshoppers is expressed in Eq. (6), in which x_i shows the location of the i^{th} insect.

$$x_i = r_1 S_i + r_2 G_i + r_3 A_i \tag{6}$$

where r_1, r_2 and r_3 represent the accidental value between intervals of 0 and 1. Also, S_i, G_i, and A_i are the social relation, the gravity force, and the wind advection, respectively. Fig. 5 is the alter that happens when grasshoppers travel and connect a large group, among other animals, in spite these mostly being seen individually [54], [55]. Also, the conceptual treatment of the comfort space and the attraction and repulsion forces between the grasshoppers is also shown in Fig. 3 and Fig.4 .

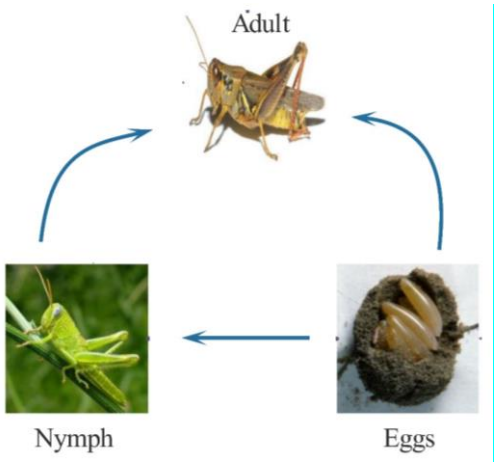

Fig. 3. The life cycle of grasshoppers [52]

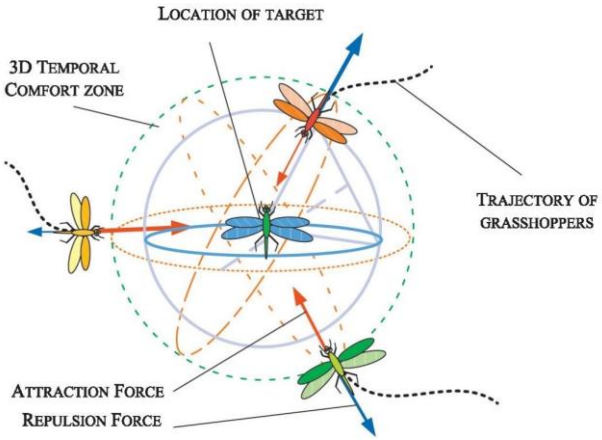

Fig. 4. Primitive corrective patterns between individuals in a swarm grasshopper [54]

2.4. Hybrid radial basis function neural network (RBFNN)

A RBFNN is recognized as a feed-forward network containing one input layer, hidden layer and output layer. Therefore, the convergence pace rate of an RBFNN is large [56]. The input nodes make a transition of input variables from the input layer to the hidden layer, which a Gaussian activation function shapes the hidden layer nodes. This type of neural network reacts to the input signals close to the center of the base function. The concluded output of the hidden layer is transmitted to the output layer, which mainly employs a simple linear function [57].

The given Fig. 5 depicts the structure of RBFNN, where $t_1, t_2, \dots, t_5$ show the network inputs and $\varphi_1, \varphi_2, \dots, \varphi_q$ depict the center of the base function in the hidden layer. As well, $w_0, w_1, \dots, w_q$ are the weights (w_0 is the output layer weight). The Gaussian function (φ) used is:

$$\varphi_i = exp\left(-\frac{\|t - c_i\|}{\sigma_i^2}\right) \quad (7)$$

φ_i Output of i^{th} node of hidden layer

c_i Prototype center of i^{th} Gaussian function

σ Spread rate parameter

$\|t - c_i\|$ Distance between input t and c_i

The output of an RBFNN could be presented via Eq. (8):

$$Y = W^T\varphi = \sum_{i=1}^{q} w_i\varphi(\|t - c_i\|) \quad (8)$$

The RBFNN is an adjustable method that automatically dedicates the spread rate and the hidden layer's neuron number. Determining parameters in the efficiency of RBFNN defines the best combination of neuron numbers and spread rate. The integrated AOA-RBFNN and GOA-RBFNN methods are applied to gain the most accurate RBFNN. The AOA and GOA algorithms determine the hidden neurons' number and the spread value to set the RBFNN structure. Hence, AOA-RBFNN and GOA-RBFNN try to build a superior model with suitable values for the above-mentioned variables.

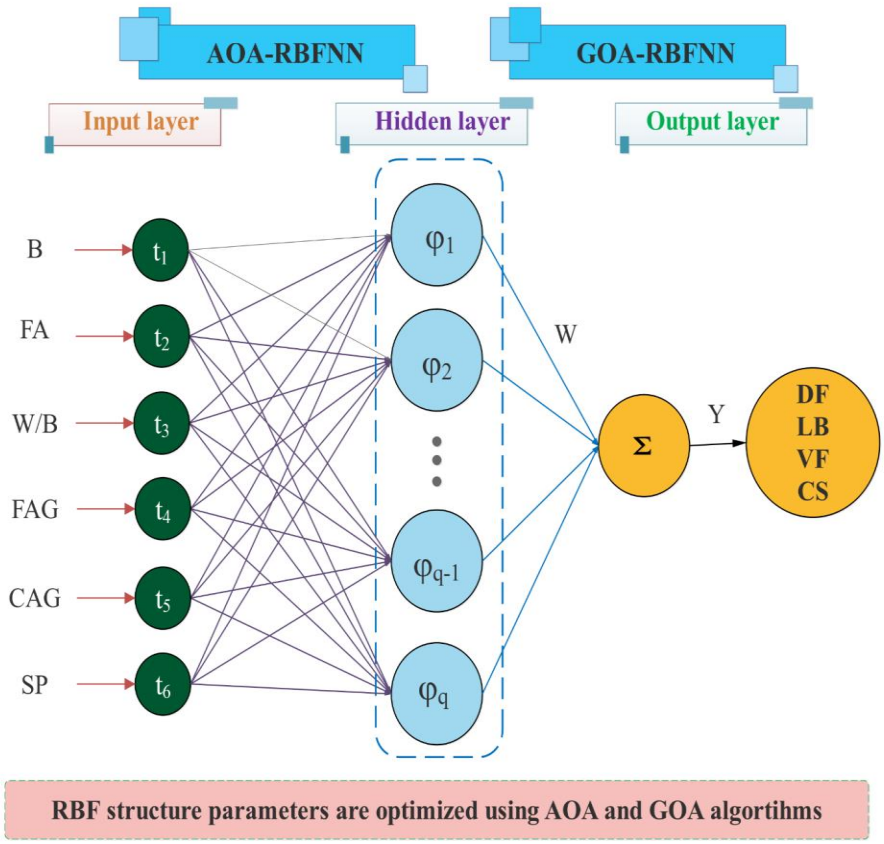

Fig. 5. Radial basis function structure

2.5. Performance evaluation indices

Different statistical performance evaluators were applied to estimate the performance of developed hybrid models for forecasting the considered properties. To this aim, Coefficient of determination (R^2), root mean squared error (RMSE), and mean absolute error (MAE), were calculated as precision measurements (Eqs. (9)-(11)):

$$R^2 = \left(\frac{\sum_{p=1}^{P}(t_P - \bar{t})(y_P - \bar{y})}{\sqrt{\left[\sum_{p=1}^{P}(t_P - \bar{t})^2\right]\left[\sum_{p=1}^{P}(y_P - \bar{y})^2\right]}} \right)^2 \quad (9)$$

$$RMSE = \sqrt{\frac{1}{P}\sum_{p=1}^{P}(y_p - t_p)^2} \quad (10)$$

$$MAE = \frac{1}{P}\sum_{p=1}^{P}|y_p - t_p| \quad (11)$$

where, y_P, t_P, $\bar{t}$, and $\bar{y}$ represent the predicted values of the P^{th} pattern, the target values of the P^{th} pattern, the averages of the target values, and the averages of the predicted values, respectively.

3. Results and Discussion

The results of the RBFNN models to forecast properties of SCC are supplied. As mentioned earlier, specifying determinative parameters in the efficiency of RBFNN is defining the best combination of spread rate and neuron numbers. The hybrid AOA-RBFNN and GOA-RBFNN models are employed for obtaining the most precise RBFNN. The optimal values of these main parameters for four properties of SCC (D flow, L-box, V-funnel, and CS) are supplied in Table 2.

Table 2. Value of RBF parameters.

Properties	RBF Parameters	AOA-RBFNN	GOA-RBFNN
D flow	Spread value	57.272	53.49

	Hidden neurons' number	75	58
	Spread value	24.98	2.432
L-box	Hidden neurons' number	75	75
	Spread value	1	57.898
V-funnel	Hidden neurons' number	75	68
	Spread value	62.701	63.733
Compressive strength	Hidden neurons' number	75	62

The supplied Fig. 5 presents powerful potential in the training and testing phase. Comparing the measurements with those forecasted by proposed models are supplied in Fig. 6 for AOA-RBFNN and GOA-RBFNN, related to hardened and fresh properties of SCC. It can be observed that the developed models have coefficient of determination in reasonable value in the learning and testing section. It means that the correlation between measured and forecasted properties of SCC from developed hybrid models is acceptable so that it represents the high accuracy in the training and approximating process.

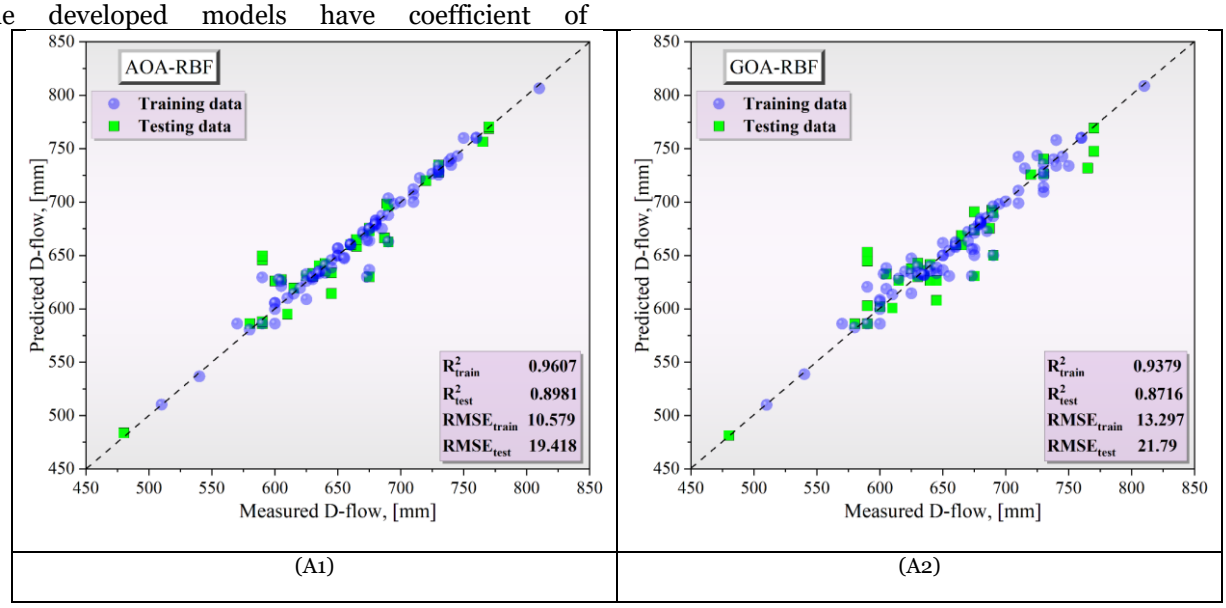

(A1) (A2)

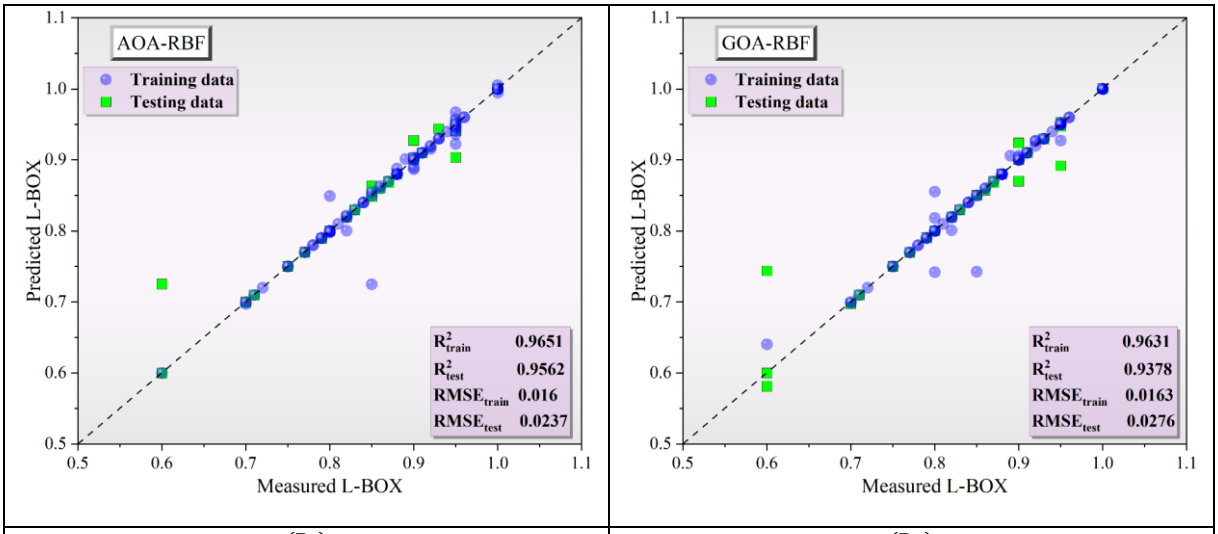

(B1)

(B2)

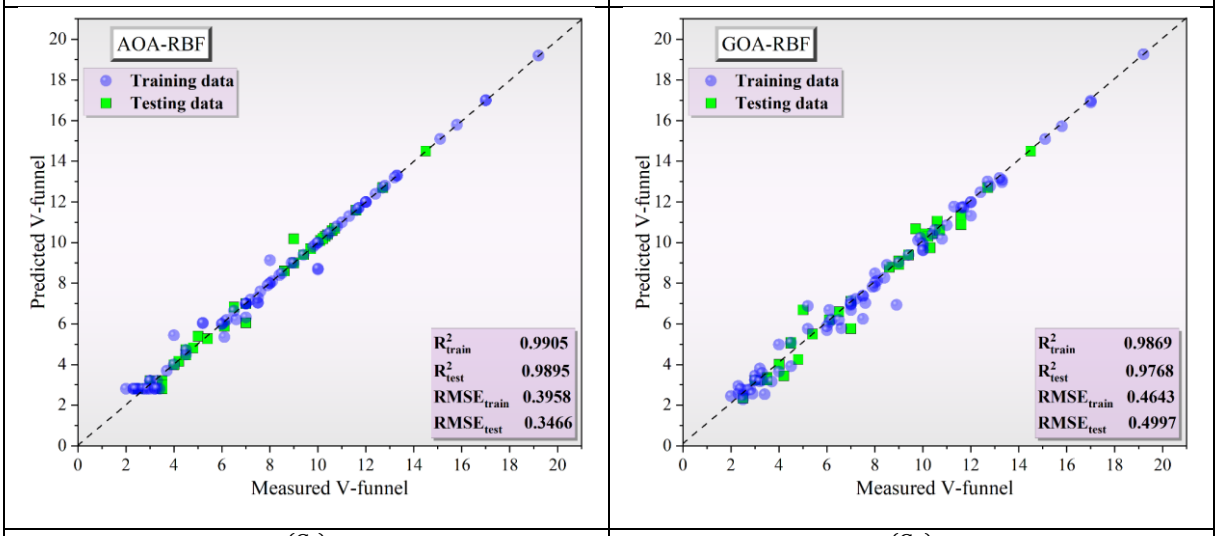

(C1)

(C2)

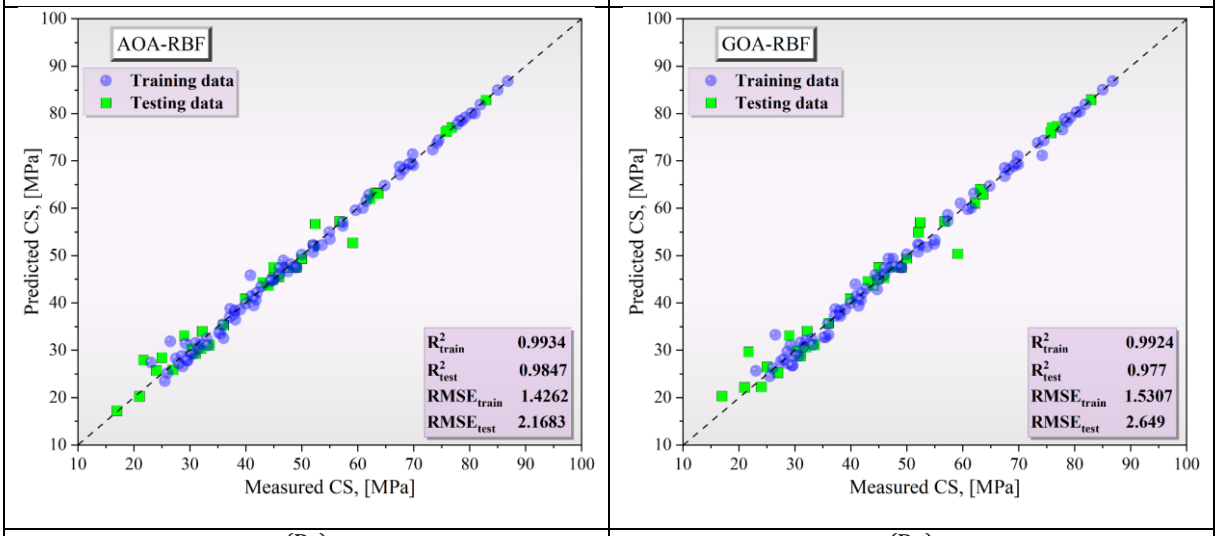

(D1)

(D2)

Fig. 6. Scatter plot between measured and predicted values

Besides, the results of developed models considering R^2, RMSE, and MAE values for fresh and hardened properties of SCC are supplied in Table 3. Along with this, the results of the proposed models in this study have been compared with the published literature [25], [26]. Regarding D flow, the results of AOA-RBFNN are better than GOA-RBFNN as well as literature. For instance, the RMSE value of model by AOA-RBFNN in the training phase is 10.579mm, while this value for GOA-RBFNN model is 13.297, followed by Saha et al. [26] at 11.67mm, and then Kaveh et al. [25] by 36.29mm.

Table 3. Statistical errors of proposed SVR models for DF.

Properties	Index	Data phase	AOA-RBF	GOA-RBF	[26]	[25]
D flow	R^2	Training data	0.9607	0.9379	0.931	0.57
		Testing data	0.8981	0.8716		
	RMSE	Training data	10.5794	13.2969	11.678	36.29
		Testing data	19.4184	21.7902		
	MAE	Training data	5.6794	8.8061		27.66
		Testing data	11.7216	14.4387		

Regarding L-box, the results of AOA-RBFNN are slightly better than GOA-RBFNN as well as literature (Table 4). For example, RMSE value of model by AOA in the training phase is 0.016, while this value for the GOA-RBFNN model is 0.0163, followed by Saha et al. [26] at 0.025, and then Kaveh et al. [25] by 0.06

Table 4. Statistical errors of proposed SVR models for LB

Properties	Index	Data phase	AOA-RBF	GOA-RBF	[26]	[25]
L-box	R^2	Training data	0.9651	0.9631	0.91	0.56
		Testing data	0.9562	0.9378		
	RMSE	Training data	0.016	0.0163	0.025	0.06
		Testing data	2.37E-02	0.0276		
	MAE	Training data	0.0046	0.0046		0.05
		Testing data	0.0073	0.0084		

Turning to V-funnel results, the results of GOA-RBFNN are moderately worse than AOA-RBFNN as well as literature (Table 5). For instance, R^2 value of model by AOA in the testing phase is 0.9895, while this value for the GOA-RBFNN model is 0.9768, followed by Saha et al. [26] at 0.958, and then Kaveh et al. [25] by 0.87.

Table 5. Statistical errors of proposed SVR models for VF

Properties	Index	Data phase	AOA-RBF	GOA-RBF	[26]	[25]
V-funnel	R^2	Training data	0.9905	0.9869	0.958	0.87
		Testing data	0.9895	0.9768		
	RMSE	Training data	0.3958	0.4643	0.723	1.46
		Testing data	0.3466	0.4997		
	MAE	Training data	0.2022	0.2989		1.11
		Testing data	0.1824	0.3303		

Finally, the result for CS is also depicts the same outputs as above (Table 6). All in all, the RBFNN model developed by AOA outperforms others, which depicts the capability of this algorithm for determining the optimal parameters of the RBFNN. But it is worth mentioning than the model developed with GOA algorithm is also powerful.

Table 6. Statistical errors of proposed SVR models FOR CS

Properties	Index	Data phase	AOA-RBF	GOA-RBF	[26]	[25]
Compressive strength	R^2	Training data	0.9934	0.9924	0.955	0.93
		Testing data	0.9847	0.977		
	RMSE	Training data	1.4262	1.5307	3.783	4.45
		Testing data	2.1683	2.649		
	MAE	Training data	0.9348	1.0667		3.45
		Testing data	1.3888	1.7529		

A justifiable correlation between observed values and forecasted values is acquirable from the time series figures

supplied in Figs. 7(a-d). As be observed, for fresh and hardened properties of SCC in AOA-RBFNN and GOA-RBFNN developed models, the measured values present appropriate agreement with predicted ones, expressing the capability of proposed hybrid algorithms to predict the D flow, L-box, V-funnel, and CS with high precision. According to time series figures, developed models result in the lowest variation in the properties predicting process, providing roughly accurate predictions which can be used for practical applications.

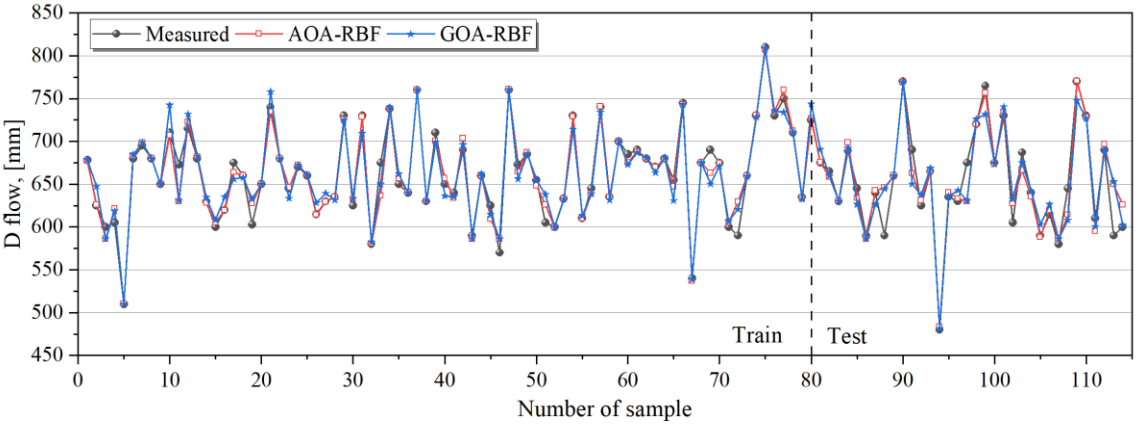

(a)

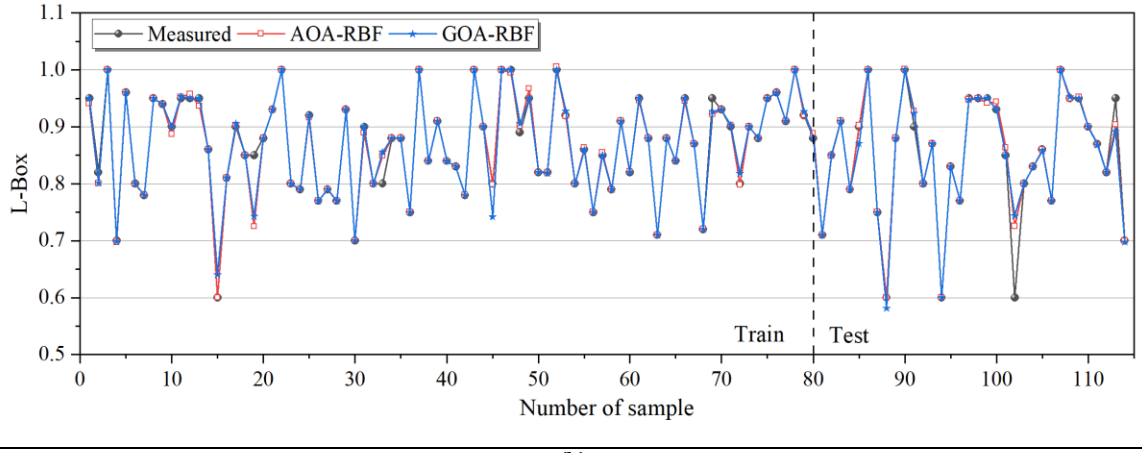

(b)

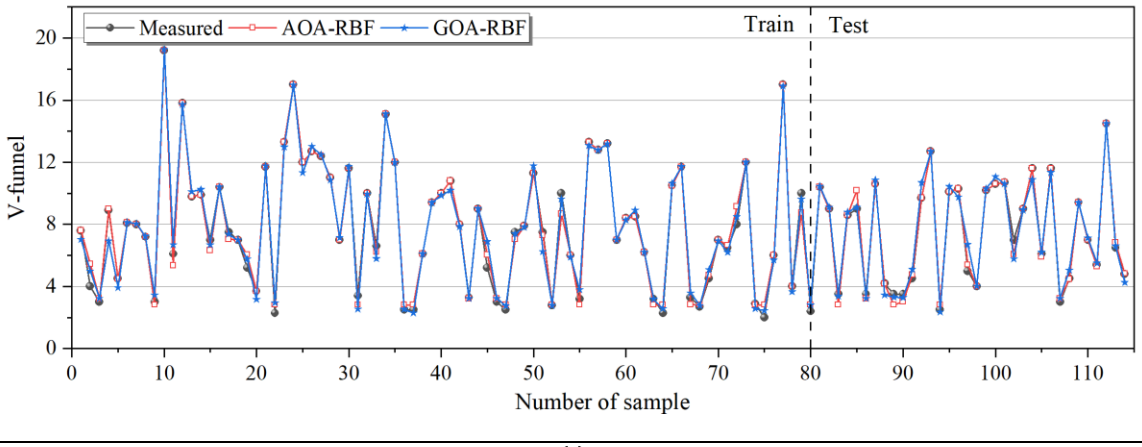

(c)

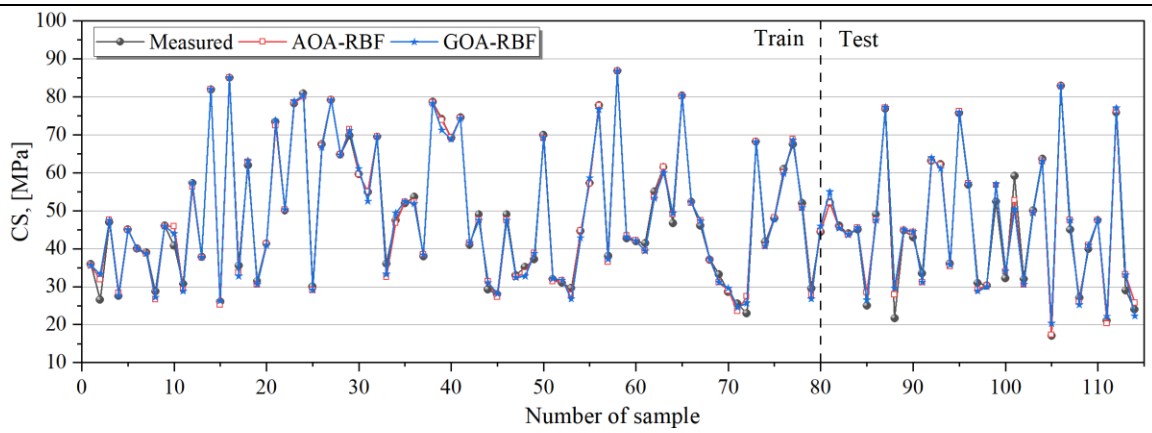

(d)

Fig. 7. Properties prediction using models for: a) D flow; b) L-Box; c) V-funnel; d) CS

4. Conclusion

It is obtained from the papers that there were restricted articles focusing on forecasting fresh or hardened properties of SCC (i.e., D flow, L-box, V-funnel, and CS). Therefore, it was tried to propose different models to predict the mechanical properties of SCC by the radial basis function neural network (RBFNN) method. The RBFNN model has determinative variables that could be optimized with algorithms, in which arithmetic optimization algorithm (AOA), and grasshopper optimization algorithm (GOA) used for this aim. Along with this, the results of the proposed models in this study have been compared with the published literature.

- The results present powerful capability during prediction process. It is observed that the developed models have coefficient of determination in reasonable value in the learning and testing section. It means that the correlation between measured and forecasted properties of SCC from developed hybrid models is acceptable so that it represents the high accuracy in the training and approximating process.
- Regarding D flow, the results of AOA-RBFNN are better than GOA-RBFNN as well as literature. For instance, the RMSE value of model by AOA-RBFNN in the training phase is 10.579mm, while this value for GOA-RBFNN model is 13.297, followed by Saha et al. [26] at 11.67mm, and then Kaveh et al. [25] by 36.29mm.
- Regarding L-box, the results of AOA-RBFNN are slightly better than GOA-RBFNN as well as literature. For example, RMSE value of model by AOA in the training phase is 0.016, while this value for the GOA-RBFNN model is 0.0163, followed by Saha et al. [26] at 0.025, and then Kaveh et al. [25] by 0.06.
- Turning to V-funnel results, the results of GOA-RBFNN are moderately worse than AOA-RBFNN as well as literature. For instance, R^2 value of model by AOA in the testing phase is 0.9895, while this value for the GOA-RBFNN model is 0.9768, followed by Saha et al. [26] at 0.958, and then Kaveh et al. [25] by 0.87. Finally, the result for CS is also depicts the same outputs as above. All in all, the RBFNN model developed by AOA outperforms others, which depicts the capability of this algorithm for determining the optimal parameters of the RBFNN. But it is worth mentioning than the model developed with GOA algorithm is also powerful.

REFERENCES

[1] J. Wang, Q. Dai, and R. Si, "Experimental and Numerical Investigation of Fracture Behaviors of Steel Fiber–Reinforced Rubber Self-Compacting Concrete," *Journal of Materials in Civil Engineering*, vol. 34, no. 1, p. 4021379, 2022.

[2] N. Garcia-Troncoso, L. Li, Q. Cheng, K. H. Mo, and T.-C. Ling, "Comparative study on the properties and high temperature resistance of self-compacting concrete with various types of recycled aggregates," *Case Studies in Construction Materials*, vol. 15, p. e00678, 2021.

[3] M. Esmaeili Falak, R. Sarkhani Benemaran, and R. Seifi, "Improvement of the Mechanical and Durability Parameters of Construction Concrete of the Qotursuyi Spa," *Concrete Research*, vol. 13, no. 2, pp. 119–134, 2020, doi: 10.22124/JCR.2020.14518.1395.

[4] I. P. Sfikas, E. G. Badogiannis, and K. G. Trezos, "Rheology and mechanical characteristics of self-compacting concrete mixtures containing metakaolin," *Constr Build Mater*, vol. 64, pp. 121–129, 2014.

[5] A. Beycioğlu and H. Y. Aruntaş, "Workability and mechanical properties of self-compacting concretes

containing LLFA, GBFS and MC," *Constr Build Mater*, vol. 73, pp. 626–635, 2014.
[6] B. Sukumar, K. Nagamani, and R. S. Raghavan, "Evaluation of strength at early ages of self-compacting concrete with high volume fly ash," *Constr Build Mater*, vol. 22, no. 7, pp. 1394–1401, 2008.
[7] M. Jalal, A. Pouladkhan, O. F. Harandi, and D. Jafari, "Comparative study on effects of Class F fly ash, nano silica and silica fume on properties of high-performance self-compacting concrete," *Constr Build Mater*, vol. 94, pp. 90–104, 2015.
[8] P. K. Acharya and S. K. Patro, "Effect of lime and ferrochrome ash (FA) as partial replacement of cement on strength, ultrasonic pulse velocity and permeability of concrete," *Constr Build Mater*, vol. 94, pp. 448–457, 2015.
[9] S.-W. Yoo, G.-S. Ryu, and J. F. Choo, "Evaluation of the effects of high-volume fly ash on the flexural behavior of reinforced concrete beams," *Constr Build Mater*, vol. 93, pp. 1132–1144, 2015.
[10] R. Sarkhani Benemaran, M. Esmaeili-Falak, and H. Katebi, "Physical and numerical modelling of pile-stabilised saturated layered slopes," *Proceedings of the Institution of Civil Engineers: Geotechnical Engineering*, pp. 1–16, 2021, doi: 10.1680/jgeen.20.00152.
[11] R. S. Benemaran and M. Esmaeili-Falak, "Optimization of cost and mechanical properties of concrete with admixtures using MARS and PSO," *Computers and Concrete*, vol. 26, no. 4, pp. 309–316, 2020, doi: 10.12989/cac.2020.26.4.309.
[12] M. Esmaeili-Falak, H. Katebi, M. Vadiati, and J. Adamowski, "Predicting triaxial compressive strength and Young's modulus of frozen sand using artificial intelligence methods," *Journal of Cold Regions Engineering*, vol. 33, no. 3, p. 4019007, 2019, doi: 10.1061/(ASCE)CR.1943-5495.0000188.
[13] A. Nassr, M. Esmaeili-Falak, H. Katebi, and A. Javadi, "A new approach to modeling the behavior of frozen soils," *Eng Geol*, vol. 246, pp. 82–90, 2018, doi: 10.1016/j.enggeo.2018.09.018.
[14] F. Özcan, C. D. Atiş, O. Karahan, E. Uncuoğlu, and H. Tanyildizi, "Comparison of artificial neural network and fuzzy logic models for prediction of long-term compressive strength of silica fume concrete," *Advances in Engineering Software*, vol. 40, no. 9, pp. 856–863, 2009.
[15] O. B. Douma, B. Boukhatem, M. Ghrici, and A. Tagnit-Hamou, "Prediction of properties of self-compacting concrete containing fly ash using artificial neural network," *Neural Comput Appl*, vol. 28, no. 1, pp. 707–718, 2017.
[16] S. Kostić and D. Vasović, "Prediction model for compressive strength of basic concrete mixture using artificial neural networks," *Neural Comput Appl*, vol. 26, no. 5, pp. 1005–1024, 2015.
[17] S. Subaşı, A. Beycioğlu, E. Sancak, and İ. Şahin, "Rule-based Mamdani type fuzzy logic model for the prediction of compressive strength of silica fume included concrete using non-destructive test results," *Neural Comput Appl*, vol. 22, no. 6, pp. 1133–1139, 2013.
[18] R. Shadi and A. Nazari, "RETRACTED ARTICLE: Predicting the effects of nanoparticles on early age compressive strength of ash-based geopolymers by artificial neural networks," *Neural Comput Appl*, vol. 31, pp. 743–750, 2019.
[19] M. Sonebi, A. Cevik, S. Grünewald, and J. Walraven, "Modelling the fresh properties of self-compacting concrete using support vector machine approach," *Constr Build Mater*, vol. 106, pp. 55–64, 2016.
[20] H. Y. Yang and Y. F. Dong, "Modelling concrete strength using support vector machines," in *Applied Mechanics and Materials*, 2013, vol. 438, pp. 170–173.
[21] J. S. Yazdi, F. Kalantary, and H. S. Yazdi, "Prediction of elastic modulus of concrete using support vector committee method," *Journal of materials in civil engineering*, vol. 25, no. 1, pp. 9–20, 2013.
[22] F. Naseri, F. Jafari, E. Mohseni, W. Tang, A. Feizbakhsh, and M. Khatibinia, "Experimental observations and SVM-based prediction of properties of polypropylene fibres reinforced self-compacting composites incorporating nano-CuO," *Constr Build Mater*, vol. 143, pp. 589–598, 2017.
[23] J. Liu, K. Yan, X. Zhao, and Y. Hu, "Prediction of autogenous shrinkage of concretes by support vector machine," *International Journal of Pavement Research and Technology*, vol. 9, no. 3, pp. 169–177, 2016.
[24] S. Yang, C. Q. Fang, and Z. J. Yuan, "Study on mechanical properties of corroded reinforced concrete using support vector machines," in *Applied Mechanics and Materials*, 2014, vol. 578, pp. 1556–1561.
[25] A. Kaveh, T. Bakhshpoori, and S. M. Hamze-Ziabari, "M5'and Mars based prediction models for properties of self-compacting concrete containing fly ash," *Periodica Polytechnica Civil Engineering*, vol. 62, no. 2, pp. 281–294, 2018.
[26] P. Saha, P. Debnath, and P. Thomas, "Prediction of fresh and hardened properties of self-compacting concrete using support vector regression approach," *Neural Comput Appl*, vol. 32, no. 12, pp. 7995–8010, 2020.
[27] J. Wang and F. Wu, "New hybrid support vector regression methods for predicting fresh and hardened properties of self-compacting concrete," *Journal of Intelligent & Fuzzy Systems*, vol. Preprint, pp. 1–15, 2022, doi: 10.3233/JIFS-220744.
[28] Z. Nurlan, "A novel hybrid radial basis function method for predicting the fresh and hardened properties of self-compacting concrete," *Advances in Engineering and Intelligence Systems*, vol. 1, no. 01, 2022.
[29] I. Aljarah, H. Faris, S. Mirjalili, and N. Al-Madi, "Training radial basis function networks using biogeography-based optimizer," *Neural Comput Appl*, vol. 29, no. 7, pp. 529–553, 2018.
[30] K. A. Rashedi, M. T. Ismail, N. N. Hamadneh, S. Wadi, J. J. Jaber, and M. Tahir, "Application of Radial Basis Function Neural Network Coupling Particle Swarm Optimization Algorithm to Classification of Saudi Arabia Stock Returns," *Journal of Mathematics*, vol. 2021, 2021.
[31] X. Liu, X. Liu, Z. Zhou, and L. Hu, "An efficient multi-objective optimization method based on the adaptive

approximation model of the radial basis function," *Structural and Multidisciplinary Optimization*, vol. 63, no. 3, pp. 1385–1403, 2021.
[32] M. Kasihmuddin, M. A. B. Mansor, S. A. Alzaeemi, and S. Sathasivam, "Satisfiability logic analysis via radial basis function neural network with artificial bee colony algorithm," *Int. J. Interact. Multimedia Artif. Intell.*.
[33] H. Wang *et al.*, "Image reconstruction for electrical impedance tomography using radial basis function neural network based on hybrid particle swarm optimization algorithm," *IEEE Sens J*, vol. 21, no. 2, pp. 1926–1934, 2020.
[34] E. M. Golafshani and G. Pazouki, "Predicting the compressive strength of self-compacting concrete containing fly ash using a hybrid artificial intelligence method," *Computers and Concrete*, vol. 22, no. 4, pp. 419–437, 2018.
[35] G. Pazouki, E. M. Golafshani, and A. Behnood, "Predicting the compressive strength of self-compacting concrete containing Class F fly ash using metaheuristic radial basis function neural network," *Structural Concrete*, 2021.
[36] R. Siddique, P. Aggarwal, and Y. Aggarwal, "Influence of water/powder ratio on strength properties of self-compacting concrete containing coal fly ash and bottom ash," *Constr Build Mater*, vol. 29, pp. 73–81, 2012.
[37] M. Şahmaran, İ. Ö. Yaman, and M. Tokyay, "Transport and mechanical properties of self-consolidating concrete with high volume fly ash," *Cem Concr Compos*, vol. 31, no. 2, pp. 99–106, 2009.
[38] Y. Aggarwal and P. Aggarwal, "Prediction of compressive strength of SCC containing bottom ash using artificial neural networks," *International Journal of Mathematical and Computational Sciences*, vol. 5, no. 5, pp. 762–767, 2011.
[39] M. Uysal and K. Yilmaz, "Effect of mineral admixtures on properties of self-compacting concrete," *Cem Concr Compos*, vol. 33, no. 7, pp. 771–776, 2011.
[40] R. Patel, "Development of statistical models to simulate and optimize self-consolidating concrete mixes incorporating high volumes of fly ash.," 2004.
[41] R. Gettu, J. Izquierdo, P. C. C. Gomes, and A. Josa, "Development of high-strength self-compacting concrete with fly ash: a four-step experimental methodology," in *Proc. 27th Conf. on Our World in Concrete & Structures, CI-Premier Pte. Ltd., Eds. CT Tam, DWS Ho, P. Paramasivam y TH Tan, Singapore*, 2002, pp. 217–224.
[42] E. Güneyisi, M. Gesoğlu, and E. Özbay, "Strength and drying shrinkage properties of self-compacting concretes incorporating multi-system blended mineral admixtures," *Constr Build Mater*, vol. 24, no. 10, pp. 1878–1887, 2010.
[43] M. C. S. Nepomuceno, L. A. Pereira-de-Oliveira, and S. M. R. Lopes, "Methodology for the mix design of self-compacting concrete using different mineral additions in binary blends of powders," *Constr Build Mater*, vol. 64, pp. 82–94, 2014.
[44] A. F. Bingöl and İ. Tohumcu, "Effects of different curing regimes on the compressive strength properties of self-compacting concrete incorporating fly ash and silica fume," *Mater Des*, vol. 51, pp. 12–18, 2013.
[45] P. Krishnapal, R. K. Yadav, and C. Rajeev, "Strength characteristics of self-compacting concrete containing fly ash," *Res J Eng Sci ISSN*, vol. 2278, p. 9472, 2013.
[46] S. Dhiyaneshwaran, P. Ramanathan, I. Baskar, and R. Venkatasubramani, "Study on durability characteristics of self-compacting concrete with fly ash," *Jordan journal of civil engineering*, vol. 7, no. 3, pp. 342–352, 2013.
[47] P. Muthupriya, P. N. Sri, M. P. Ramanathan, and R. Venkatasubramani, "Strength and workability character of self-compacting concrete with GGBFS, FA and SF," *Int J Emerg Trends Eng Dev*, vol. 2, no. 2, pp. 424–434, 2012.
[48] B. Mahalingam and K. Nagamani, "Effect of processed fly ash on fresh and hardened properties of self-compacting concrete," *Int J Earth Sci Eng*, vol. 4, no. 5, pp. 930–940, 2011.
[49] P. Debnath and A. K. Dey, "Prediction of bearing capacity of geogrid-reinforced stone columns using support vector regression," *International Journal of Geomechanics*, vol. 18, no. 2, p. 4017147, 2018.
[50] L. Abualigah, A. Diabat, S. Mirjalili, M. Abd Elaziz, and A. H. Gandomi, "The arithmetic optimization algorithm," *Comput Methods Appl Mech Eng*, vol. 376, p. 113609, 2021, doi: 10.1016/j.cma.2020.113609.
[51] S. J. Simpson, A. R. McCAFFERY, and B. F. Hägele, "A behavioural analysis of phase change in the desert locust," *Biological reviews*, vol. 74, no. 4, pp. 461–480, 1999.
[52] S. Saremi, S. Mirjalili, and A. Lewis, "Grasshopper optimisation algorithm: theory and application," *Advances in Engineering Software*, vol. 105, pp. 30–47, 2017.
[53] M. Mafarja, I. Aljarah, H. Faris, A. I. Hammouri, A.-Z. Ala'M, and S. Mirjalili, "Binary grasshopper optimisation algorithm approaches for feature selection problems," *Expert Syst Appl*, vol. 117, pp. 267–286, 2019.
[54] M. Mafarja *et al.*, "Evolutionary population dynamics and grasshopper optimization approaches for feature selection problems," *Knowl Based Syst*, vol. 145, pp. 25–45, 2018.
[55] Y. Gad, H. Diab, M. Abdelsalam, and Y. Galal, "Smart Energy Management System of Environmentally Friendly Microgrid Based on Grasshopper Optimization Technique," *Energies (Basel)*, vol. 13, no. 19, p. 5000, 2020.
[56] W. Sun, D. Liu, J. Wen, and Z. Wu, "Modeling of MEMS gyroscope random errors based on grey model and RBF neural network," *J. Navig. Position*, vol. 5, pp. 9–13, 2017.
[57] S. Seshagiri and H. K. Khalil, "Output feedback control of nonlinear systems using RBF neural networks," *IEEE Trans Neural Netw*, vol. 11, no. 1, pp. 69–79, 2000.